Full Length Article

Degradation of two novel congenital TTP ADAMTS13 mutants by the cell proteasome prevents ADAMTS13 secretion

Mary Underwood [a,b,*,1], Flora Peyvandi [a,b,c], Isabella Garagiola [c], Samuel Machin [a], Ian Mackie [a]

[a] Haemostasis Research Unit, University College London, London, England
[b] Department of Pathophysiology and Transplantation, University of Milan, Milan, Italy
[c] Angelo Bianchi Bonomi Hemophilia and Thrombosis Centre, Fondazione IRCCS Ca' Granda Ospedale Maggiore Policlinico, Milan, Italy

ABSTRACT

Introduction: Over 150 mutations have been identified in the ADAMTS13 gene in patients with congenital thrombotic thrombocytopenic purpura (TTP). The majority of these (86%), lead to reduced (<50%) secretion of mutant recombinant ADAMTS13. The mechanism by which this occurs has not been investigated in vitro. Two novel ADAMTS13 mutations (p.I143T and p.Y570C) identified in two congenital adolescence onset TTP patients were studied, to investigate their effects on ADAMTS13 secretion and subcellular localisation.
Materials and Methods: HEK293T cells were transiently transfected with wild type or mutant ADAMTS13 cDNA. Immunofluorescence and confocal microscopy were used to study localisation within the endoplasmic reticulum (ER) and Golgi. The cell proteasome and lysosomes were inhibited in cells stably expressing ADAMTS13 to investigate degradation of ADAMTS13 by either organelle.
Results: Both mutations severely impaired secretion and both mutants localised within the ER and Golgi. Proteasome inhibition led to the intracellular accumulation of both mutants, suggesting proteasome degradation. Lysosome inhibition on the other hand did not lead to increased intracellular accumulation of the mutants.
Conclusions: Proteasome degradation of these ADAMTS13 mutants contributed to their reduced secretion.

© 2016 Elsevier Ltd. All rights reserved.

1. Introduction

Thrombotic thrombocytopenic purpura (TTP) patients have an acquired or congenital deficiency in ADAMTS13 activity [1–3]. ADAMTS13 processes and cleaves Von Willebrand factor (VWF) at the Tyr1605-Met1606 peptide bond in the A2 domain [4,5]. Its deficiency leads to the accumulation of ultra-large VWF (ULVWF) multimers within the circulation, leading to the uncontrolled formation of platelet-rich thrombi in the microcirculation and subsequent vessel occlusion.

Congenital TTP patients are presently treated with plasma infusion/exchange which provides a source of ADAMTS13. Despite these patients typically having severely reduced ADAMTS13 activity, the clinical presentation and response to treatment is highly variable. Evidence suggests that the ADAMTS13 genotype may account for some of this heterogeneity. Over 150 mutations have been identified throughout the ADAMTS13 gene in patients with congenital TTP [1,6–19] and relationships appear to exist between ADAMTS13 genotype, age of disease onset [20] and residual ADAMTS13 activity [11]. Residual ADAMTS13

activity in turn appears to be associated with the annual rate of TTP episodes and with the requirements for fresh frozen plasma prophylaxis [11].

As residual ADAMTS13 activity appears to be associated with disease severity and with ADAMTS13 genotype, it is important to understand how different ADAMTS13 mutations affect its function. Of the mutations identified, approximately 30% have been expressed in vitro [7,20–22]. These mutations affect to various degrees the secretion and activity of ADAMTS13 [20]. The majority (86%), lead to reduced (<50% of wild type [WT]) secretion of mutant recombinant ADAMTS13, suggesting misfolding of ADAMTS13 and subsequent retention and degradation by the cell. The mechanism by which this may occur however has not been investigated in vitro.

With this in mind we studied two novel previously uncharacterised mutations (p.I143T, p.Y570C) present in a homozygous form in two different congenital TTP patients [17,23]. Both of these mutations are located within the N-terminal region of ADAMTS13. The p.I143T mutation is located within the metalloprotease domain which contains the catalytic site necessary for VWF cleavage [24]. The p.Y570C mutation localises within the spacer domain which is important for VWF binding [25–27]. The clinical history of both patients has been described previously [17], but in brief both presented with acute TTP during adolescence with undetectable ADAMTS13 activity and antigen and both receive prophylactic plasma infusion every three to four weeks. The effect of

these mutations on ADAMTS13 secretion was assessed along with their effect on the intracellular localisation of ADAMTS13.

2. Materials and Methods

All reagents were obtained from Sigma Aldrich Chemical Company Ltd. (Poole, UK) unless stated otherwise.

2.1. Site Directed Mutagenesis

The p.I143T (c.428 T > C) and p.Y570C (c.1709 A > G) ADAMTS13 mutations were introduced by site directed mutagenesis into a pcDNA 3.1/V5-His TOPO® vector (Life technologies, Paisley, UK) containing the complete ADAMTS13 cDNA as previously described [28], primers are available upon request.

2.2. Transient and Stable Line Expression

HEK 293T cells were transiently transfected with WT or mutant ADAMTS13 cDNA as previously described [21], along with 1 μl of pRL-TK plasmid (Promega, Southampton, UK) to normalize the transfection efficiency. The pRL-TK vector expresses Renilla luciferase which produces luminescence in the presence of its substrate (luminol). The Renilla luciferase assay system (Promega) was used to measure luminescence in cell lysate samples according to the manufacturer's recommendations. The luminescence values were used to normalize antigen and activity results. DMEM media was exchanged for OptiMEM media just before transfection. Supernatant and cell lysate samples were harvested four days after transfection as previously described [28].

Stable lines expressing WT or mutant ADAMTS13 were created as previously described [28]. WT and mutant supernatant from transiently transfected cells was concentrated ~20 fold, whereas WT and mutant supernatant from stable lines were concentrated ~100 fold using centrifugal filter devices with a 100 kDa cut-off (Millipore UK Ltd., Livingston, UK).

2.3. Western Blotting

For SDS-PAGE on transient transfection samples, the volumes loaded were normalized according to the transfection efficiency. Samples were loaded onto 4–12% Bis-Tris polyacrylamide gels (Bio-Rad Laboratories Ltd., Hemel Hempstead, UK) and protein was transferred onto 0.45 μm nitrocellulose membranes (GE Healthcare, Little Chalfont, UK). A primary mouse anti-V5 monoclonal antibody (Life technologies) against the C-terminal V5 tag expressed by the recombinant protein was used, followed by an ECL anti-mouse IgG HRP secondary antibody (GE Healthcare) for supernatant samples. For cell lysate samples membranes were also incubated with an anti β actin antibody loading control (Abcam, Cambridge, UK) after proteasome and lysosome inhibition. Membranes were developed using supersignal west pico chemiluminescent substrate (Fisher Scientific, Loughborough, UK) followed by exposure onto Amersham Hyperfilm ECL (GE Healthcare).

2.4. ADAMTS13 Antigen and Activity

ADAMTS13 antigen in supernatant samples from transiently transfected cells was measured using an in house ADAMTS13 antigen ELISA [29] (detection limit 3% of pooled normal plasma (PNP). ADAMTS13 antigen in supernatant samples from proteasome and lysosome inhibition experiments was measured using an Imubind ADAMTS13 antigen ELISA (Sekisui Diagnostics, Stamford, USA) (detection limit <60 ng/ml, ~6% PNP) as one of the antibodies for the in house ELISA is no longer commercially available. ADAMTS13 activity in supernatant samples was measured using FRETS-VWF73 as substrate [30] with minor modifications [31] (detection limit 5% of PNP).

2.5. Confocal Microscopy

ADAMTS13 localisation within the cell endoplasmic reticulum (ER) and Golgi was investigated using immunofluorescent labelling and confocal microscopy, with antibodies directed against ADAMTS13 and either the ER or Golgi. HEK 293T cells transiently transfected with ADAMTS13 cDNA were fixed with 4% paraformaldehyde, permeabilised with 0.2% Triton and blocked overnight with 3% BSA containing 0.3 M glycine. A chicken anti-V5 primary antibody (Cambridge Biosciences Ltd., Cambridge, UK) and either a mouse anti-GM130 (BD Biosciences, Oxford, UK, cis Golgi marker) or a mouse anti-PDI (protein disulphide isomerase) primary antibody (RL90 Abcam, Cambridge, UK, ER marker) was used. A rabbit FITC conjugated anti-chicken antibody (Life technologies) was used to detect the primary anti-V5 antibody. A goat Cy3 conjugated anti-mouse antibody (Millipore UK Ltd) was used to detect the ER/Golgi primary antibody. Cells were mounted with Vectashield® mounting media containing DAPI to stain for nuclei (Vector Laboratories Ltd., Peterborough, UK). Four to six slides were imaged per experiment, over an area of 4.84cm^2.

Cells were viewed at room temperature using a spinning disk confocal microscope (Perkin Elmer, Massachusetts, USA) with a Volocity acquisition system, built on a Zeiss inverted microscope. Images were captured using either a ×63 or ×100 immersion oil objective both with a 1.4 numerical aperture. Wavelengths for excitation vs. emission were as follows: DAPI, 405 nm vs. 455/460 nm; FITC, 488 nm vs. 527/555 nm and Cy3 568 nm vs. 615/670 nm.

2.6. Quantitation of Cis Golgi Colocalisation

The degree of colocalisation between ADAMTS13 and the cis Golgi was quantified using Volocity 3D analysis software (Perkin Elmer). Clearly defined cells containing unsaturated voxels (throughout the Z-stack) were used for analysis. The threshold Pearson Correlation Coefficient (TPCC) [32] and M_1 Manders overlap colocalisation coefficient (M_1) [32,33] were measured. For both types of analysis a 'threshold' was set to exclude background voxels, only voxels above this threshold were used for analysis. This was set by selecting a region containing no cells, the average voxel intensities within this region of interest plus 3 standard deviations was then calculated by the software. Threshold values for each channel (FITC: 527/555 nm, Cy3:515/670 nm) were calculated separately. The same threshold values were used throughout the analysis. Images from three separate experiments were used for analysis. Analysis was restricted to regions containing ADAMTS13 expressing cells. The numbers of cells analysed were as follows: WT (n = 35), p.I143T (n = 29) and p.Y570C (n = 52). Values are expressed as mean ± SEM.

The TPCC gives a value for the correlation between the intensity distributions of the components (Golgi and ADAMTS13) whereas the overlap between the intensities can be described by the coefficient M_1. Here M_1 represents the sum of the intensities of the 'red' Golgi expressing voxels which are colocalised with the green ADAMTS13 voxels divided by the sum of the intensities of all the red (Golgi) voxels [32,33].

2.7. Proteasome and Lysosome Inhibition

Proteasome and lysosomes were inhibited initially in HEK 293T cells transiently transfected with WT or mutant ADAMTS13. However the results from this were unreliable due to differences in the transfection efficiency which could not be normalized using the pRL-TK vector. Instead HEK 293 cells stably expressing WT or mutant ADAMTS13 cDNA were incubated with either 10 μM MG132 (Merck Chemicals, Nottingham UK), 6 μM ALLN (Merck chemicals, prepared in DMSO), 0.1 μM Bafilomycin A1 (prepared in DMSO), or 0.1% DMSO (volume added equivalent to greatest volume of drug added). DMEM media was exchanged for OptiMEM media prior to inhibitor incubation. After 5 h cell lysate and supernatant samples were harvested and analysed. The

ADAMTS13 antigen and activity measured in the supernatant in the presence of inhibitors or DMSO in a given experiment were expressed as a proportion of the values measured in the absence of any inhibitor or DMSO to normalize the results. WT and mutant values in the absence of inhibitor and DMSO i.e. 'control', was arbitrarily chosen as 1. The mean $\pm$ SEM of these normalized values are shown.

2.8. Densitometry

Densitometry was used to quantify the amount of ADAMTS13 within cell lysate samples after proteasome or lysosome inhibition. Image J software was used for analysis (http://imagej.nih.gov/ij/).

2.9. Statistical Analysis

Unpaired two-tailed Student's t-tests were used for analysis of differences between colocalisation coefficients, when the mean of WT and mutant coefficients were compared. For statistical analysis of normalized data (antigen, activity and densitometry), differences between the mean of normalized data and a hypothesised mean of 1 (i.e. no difference) were tested. A probability (p) value of <0.05 was considered significant.

3. Results

3.1. Transient Transfection

ADAMTS13 was detected within the cell lysates of WT and mutant transiently transfected cells (Fig. 1A). No ADAMTS13 protein could be detected in the cell supernatant using western blotting (Fig. 1B) or an ADAMTS13 antigen ELISA and consequently no activity could be detected. Under similar conditions WT ADAMTS13 antigen (n = 3) was 96% (633 ng/ml) (WT and mutant transfected cells were treated in the same way, data was normalized to take into account the transfection efficiency, i.e. number of cells transfected, WT and mutant supernatant harvested after the same amount of time and both concentrated 20 fold).

3.2. Confocal Microscopy

As both mutants appeared to be synthesised within the cell, but secreted at a severely reduced level, their localisation within elements of the secretion pathway was investigated. WT and mutant ADAMTS13

localised extensively within the ER (Fig. 2A). Similarly WT ADAMTS13 localised within the *cis* Golgi (Fig. 2B), as did both mutants. However the degree of localisation in the *cis* Golgi appeared to be less extensive for the mutants compared to WT.
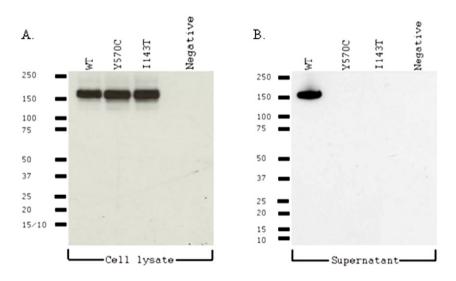
Subsequently the degree of colocalisation between the *cis* Golgi and WT or mutant ADAMTS13 was quantified. TPCC values were slightly lower for the mutants (p.I143T: 0.20 ± 0.016; p.Y570C: 0.20 ± 0.011) compared to WT (0.27 ± 0.013). These differences were statistically significant for both the p.I143T (P = 0.0009) and p.Y570C mutants (P = 0.0002). Similarly, the mean M_1 coefficient was slightly lower (p.I143T: 0.87 ± 0.024; p.Y570C: 0.81 ± 0.023) for both mutants compared to WT (0.89 ± 0.027). This difference was statistically significant for the p.Y570C mutant (P = 0.0167) but not the p.I143T mutant (P = 0.4650).

3.3. Proteasome and Lysosome Inhibition

As both mutants appeared to be synthesised within the cell, localised within the ER and to some extent within the Golgi, but did not appear to be secreted from the cells, we hypothesised that the misfolded mutants were targeted for degradation within the cell, thereby preventing secretion. HEK 293 cells stably expressing WT or mutant ADAMTS13 were incubated with proteasome or lysosome inhibitors.

Addition of the proteasome inhibitor MG132 [34] to cells stably expressing both mutants led to an increase in the intracellular levels of ADAMTS13 (Fig. 3A, B), densitometric analysis revealed an increase of $19 \pm 2\%$ for the p.I143T mutant and $38 \pm 10\%$ for the p.Y570C mutant (Table 1). This difference was statistically significant for the p.I143T mutant. This increase was not observed in cells stably expressing WT ADAMTS13 ($87 \pm 8\%$ of control). Addition of the calpain, cathepsin, cysteine protease and proteasome inhibitor ALLN [34], led to a slight non-significant increase in intracellular levels for the p.I143T mutant ($15 \pm 8\%$ increase), but not the p.Y570C mutant ($3 \pm 1\%$ increase). Addition of the lysosome inhibitor Bafilomycin A1 [35] led to an increase in WT ADAMTS13 intracellular levels ($24 \pm 11\%$ increase). However the same increase was not observed for the two mutants (~90% of control). DMSO was added to the cells as a control because it was the solvent for all inhibitors. DMSO has been shown to act as a chaperone, aiding protein folding [36–38]. In the presence of DMSO intracellular levels of WT and mutant ADAMTS13 did not increase.

The quantity of WT and mutant ADAMTS13 protein was measured in the supernatant of stably transfected cells in the presence of proteasome or lysosome inhibitors. In these experiments the supernatant was
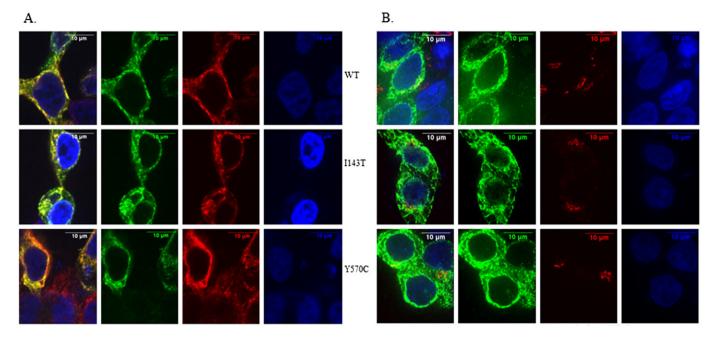

Fig. 1. Western blot analysis of cell lysate and cell supernatant samples harvested from HEK293T cells transiently expressing WT, p.Y570C or p.I143T mutant ADAMTS13. Cell lysate (A) and supernatant (B) samples were harvested 96 h after transfection. Samples were loaded onto 4–12% Bis-Tris polyacrylamide gels. WT and mutant supernatant was concentrated ~20 fold for analysis. ADAMTS13 expected size ~190 kDa. Results shown are representative of three experiments.

Fig. 2. Localisation of WT and mutant (p.I143T, p.Y570C) ADAMTS13 within the cell ER or *cis* Golgi as demonstrated by confocal microscopy. ADAMTS13 localisation in the ER (A) and *cis* Golgi (B) is shown. Cells were viewed using a Perkin Elmer Ultraview spinning disk confocal microscope at room temperature and images were acquired using Hamamatsu 9100-500 camera and Volocity software. Cells were mounted with Vectashield mounting media (Vector laboratories). FITC labelled ADAMTS13 is shown in green, Cy3 labelled ER or Golgi in red, DAPI labelled nuclei in blue and a merged image of all channels is shown on the far left to demonstrate colocalisation. Cells shown in A were viewed with an original magnification of ×630, numerical aperture 1.4, cells in B with an original magnification of ×1000, numerical aperture 1.4.

concentrated to a greater degree (~100 fold) than in the transient transfections; the p.I143T and particularly the p.Y570C mutant could be detected in the supernatant in some of these experiments. The ADAMTS13 antigen and activity measured in replicate experiments under the same conditions varied slightly, therefore the results were normalized. There were no consistent changes in WT ADAMTS13 antigen and activity measured in the supernatant after the addition of either proteasome inhibitor (MG132 or ALLN) (antigen MG132 and ALLN: 1.1 ± 0.2, activity MG132: 1.3 ± 0.5, activity ALLN: 1.2 ± 0.2) (Fig. 4A, B).

In contrast, ADAMTS13 activity levels appeared to be slightly higher in the presence of MG132 for the p.I143T (activity: 1.8 ± 0.6) and particularly for the p.Y570C secretion defect mutant (antigen: 1.7 ± 0.5, activity: 2.8 ± 1.1) (Fig. 4D-F). ALLN appeared to cause a slight average increase in ADAMTS13 activity for the p.I143T mutant (1.4 ± 0.4) (Fig. 4D), but not to the extent observed with MG132. Similarly for the p.Y570C mutant a slight increase in ADAMTS13 levels was observed (antigen: 1.3 ± 0.6, activity: 1.6 ± 1.2) (Fig. 4E, F) in the presence of ALLN, but experimental variability was higher. However these differences were not statistically significant. The addition of Bafilomycin A1 led to a decrease in ADAMTS13 levels for both WT and mutant protein (Fig. 3C, D, 4). This difference was statistically significant for the p.Y570C mutant.

DMSO led to a variable, but consistent increase in WT ADAMTS13 secretion (antigen: 2.4 ± 1.1, activity: 2.5 ± 1.3). For the p.I143T mutant ADAMTS13 activity increased slightly with DMSO, but not to the extent observed with WT (1.5 ± 0.4). The p.I143T antigen and activity values measured in these experiments were close to the detection limit of the assays used to measure them. In contrast for the p.Y570C mutant average antigen and activity levels measured in the presence of DMSO were slightly lower compared to in its absence (antigen 0.8 ± 0.4, activity 0.5 ± 0.2) (Fig. 4E, F).

In the above described experiments 'WT control' antigen and activity levels were 472 ± 94 ng/ml and $50 \pm 11\%$ (mean $\pm$ SEM). Mutant 'p.I143T control' antigen could be detected in 1 of 3 experiments (60 ng/ml) and 'p.I143T control' activity could be measured in two

experiments, values were $7 \pm 2\%$. Mutant 'p.Y570C control' antigen and activity values were 258 ± 67 ng/ml and $11 \pm 5\%$ respectively, (mean $\pm$ SEM).

4. Discussion

Studies of the impact of the *ADAMTS13* mutations found in congenital TTP on protein function are important as certain mutations may be associated with a higher degree of protein misfolding and/or secretion defect and have a more severe clinical phenotype. Greater understanding of the effect of various mutations on protein secretion and function may contribute to changes in patient management, prophylaxis and therapy.

We have studied two mutations present in a homozygous state in two congenital TTP patients who first presented with disease during adolescence and now require plasma infusion every three to four weeks [17]. The p.I143T mutation present in patient one is situated within the metalloprotease domain, which contains the catalytic site necessary for VWF cleavage. The p.Y570C mutation present in patient two is located within the spacer domain, which is important for VWF binding [25–27]. This amino acid forms part of the surface aromatic cluster on the outer surface of a beta sheet [39]. *In vitro* expression of these mutations showed that they both severely impaired the secretion of ADAMTS13; no ADAMTS13 antigen or activity could be detected in the supernatant harvested after transient transfection, even after concentrating ~20 fold. After concentration, WT ADAMTS13 antigen levels in this experimental system were similar to those found in PNP (average 96% of PNP, 633 ng/ml). These *in vitro* results were in agreement with the fact that ADAMTS13 antigen and activity were undetectable in the patient's plasma (<1% PNP) [11,17].

In order to study the intracellular processing of the mutant proteins, immunofluorescence confocal microscopy and proteasome/lysosome inhibition experiments were performed. Secretory proteins journey through the ER and Golgi where they undergo post-translational modification and folding. Confocal microscopy demonstrated that WT and mutant ADAMTS13 localised within the ER and the *cis* Golgi.
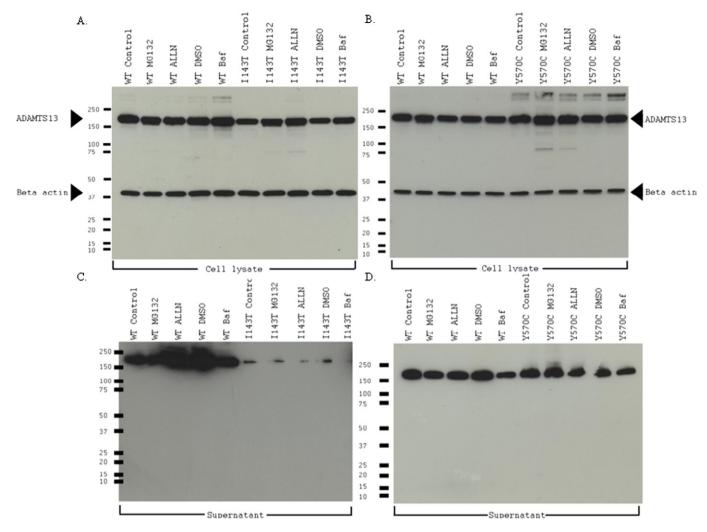
Fig. 3. Western blot analysis of cell lysate and cell supernatant samples harvested from HEK293 cells stably expressing either WT or mutant ADAMTS13, incubated in the presence of proteasome or lysosome inhibitors. (A) WT and p.I143T cell lysates, (B) WT and p.Y570C cell lysates. (C) WT and p.I143T supernatant and (D) WT and p.Y570C supernatant samples were harvested ~5 h after the addition of proteasome or lysosome inhibitors. HEK 293 cells stably expressing WT or mutant ADAMTS13 were incubated with proteasome inhibitors MG132 and ALLN or the lysosome inhibitor Bafilomycin A (Baf). The cells were also incubated with DMSO as a negative control. WT and mutant supernatant was concentrated ~100 fold for analysis. ADAMTS13 expected size ~190 kDa, β actin ~42 kDa. 'Control' indicates samples harvested from cells incubated in the absence of MG132, ALLN, Bafilomycin or DMSO. Western blots are representative of three experiments.

Localisation of the mutants in the *cis* Golgi appeared to be less extensive for the mutants and so we attempted to quantify differences in the localisation between the *cis* Golgi and WT or mutant protein.

Table 1

ADAMTS13 intracellular levels in cell lysates. Densitometry was used to measure ADAMTS13 levels in cell lysates after western blotting. Mean ± SEM are shown for each condition. Values are expressed as a proportion of control, arbitrarily assigned a value of 1. P values obtained after Student's *t*-test analysis are shown, **<0.01.

	Condition	ADAMTS13 levels	P value
WT	Control	1	–
	MG132	0.87 ± 0.08	0.187
	ALLN	0.96 ± 0.09	0.643
	DMSO	1.03 ± 0.10	0.774
	Bafilomycin	1.24 ± 0.11	0.077
I143T	Control	1	–
	MG132	1.19 ± 0.02	0.005**
	ALLN	1.15 ± 0.08	0.149
	DMSO	1.05 ± 0.04	0.295
	Bafilomycin	0.90 ± 0.09	0.346
Y570C	Control	1	–
	MG132	1.38 ± 0.10	0.070
	ALLN	1.03 ± 0.01	0.169
	DMSO	0.89 ± 0.03	0.060
	Bafilomycin	0.96 ± 0.03	0.253

Quantitative analysis revealed statistical differences between WT and mutant TPCC suggesting reduced correlation between ADAMTS13 and the *cis* Golgi in the mutants. There was a significant difference between the M_1 coefficient for WT and the p.Y570C mutant, suggesting that there was reduced overlap between the *cis* Golgi and ADAMTS13 in this mutant. There was a large variation in the measured TPCC and M_1 in the individual cells analysed. Perhaps to detect significant differences between the M1 coefficient and WT and the p.I143T mutant a larger number of cells would need to be analysed.

Transiently transfected cells were used for confocal microscopy because stable line cells were not available at the time of analysis. One of the weaknesses of using transiently transfected cells is that the level of expression in each transiently transfected cell may differ. Consequently both high and low expressing cells were included in the quantitation analysis. Low expressing cells can have higher colocalisation [40] possibly because the higher concentrations of fluorescent protein saturates high affinity sites and also occupy sites with lower affinities, whereas lower concentrations are confined to the high affinity sites [41]. This may account for the variability in the colocalisation coefficients measured in different cells expressing the same ADAMTS13 form (i.e. WT or mutant).

Misfolded or aggregated proteins are targeted to the proteasome or lysosomes for degradation [42] and so we investigated whether the
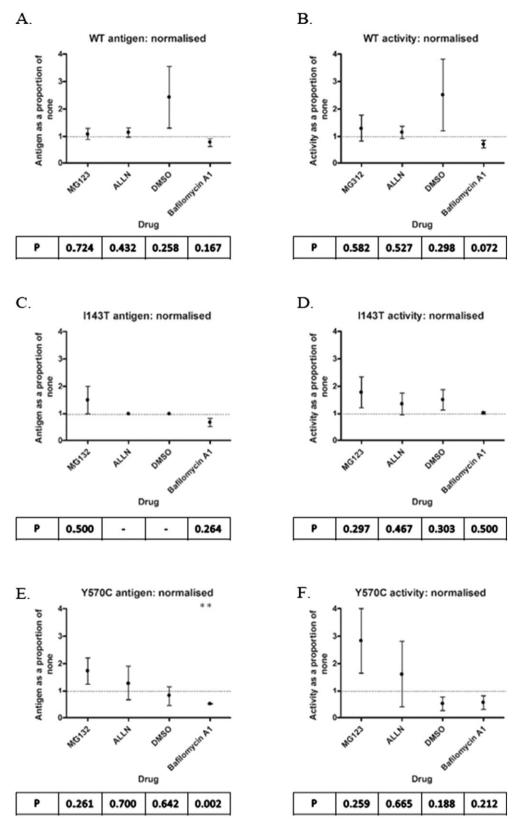
Fig. 4. ADAMTS13 antigen and activity measured in supernatant samples. Values are represented as mean + SEM. For analysis of WT, n = 7 and for the mutants n = 3. The dotted line indicates values in the absence of inhibitor and DMSO, i.e. 1. Half the detection limit (2.5%) was used in the analysis for samples from some experiments where ADAMTS13 levels for the p.I143T mutant and p.Y570C mutant were below the detection limit (5%), in order to calculate mean values. Student's t-test P values are shown below each diagram, **<0.01.

mutants were degraded by either organelle. Proteasome inhibition using MG132 led to increased intracellular levels of both mutants. These results indicate that degradation of the mutants occurs in the proteasome whereas WT ADAMTS13 showed no significant degradation by

this route. Targeting of the mutant to the proteasome for degradation would prevent its secretion from the cell. ALLN is a calpain, cathepsin, cysteine protease and proteasome inhibitor [34]. MG132 and ALLN have been shown to increase intracellular levels of other proteins [43,

44], however only MG132 was shown to increase the mutant ADAMTS13 levels, this may be because it is a more specific proteasome inhibitor, compared to ALLN.

Increased intracellular levels of WT ADAMTS13 could be measured after treating HEK 293 cells with Bafilomycin A1, suggesting that a proportion of WT ADAMTS13 is degraded by lysosomes. These organelles unlike proteasomes predominantly degrade aggregated proteins [45] suggesting that some WT ADAMTS13 may be aggregated within the cell, this could be due to the high levels of ADAMTS13 expressed within the HEK 293 cells used in this system. The vector expressing *ADAMTS13* contained a CMV promoter which would result in high ADAMTS13 levels, perhaps greater than physiological levels. Aggregation of WT ADAMTS13 may be due to the system used to express ADAMTS13 rather than this being a normal feature of ADAMTS13 synthesis. There did not appear to be increased levels of the mutants within the cell after lysosome inhibition suggesting that this organelle is not a significant degradation route for these proteins. It is possible that the mutant proteins were degraded by the proteasome before they had the opportunity to aggregate, or that the structural changes introduced by the mutations prevented their aggregation.

Proteasome inhibition appeared to lead to a slight increase in the levels of the p.I143T mutant, however these differences were small and levels of p.I143T antigen and activity in these experiments were very close to the detection limit. With the p.Y570C mutant a marked increase in levels after the addition of MG132 could be observed. MG132 has been shown to activate the unfolded protein response, which leads to an increase in chaperones and folding enzymes to enhance the folding of misfolded proteins [46]. Furthermore perhaps by inhibiting the proteasome, there was longer retention of the mutant within the ER or Golgi, which would have led to a greater amount of time in which the protein could fold and be subsequently secreted.

4.1. Conclusions

Both the p.I143T and p.Y570C mutations severely impaired ADAMTS13 secretion. The mutants were synthesised within the cell and localised within elements of the secretion pathway (ER and Golgi) suggesting that progress from the Golgi was impeded. The misfolded mutants appeared to be predominantly degraded by the proteasome as intracellular levels increased in the presence of proteasome inhibitors.

Acknowledgements

References

[1] G.G. Levy, W.C. Nichols, E.C. Lian, T. Foroud, J.N. McClintick, B.M. McGee, A.Y. Yang, D.R. Siemieniak, K.R. Stark, R. Gruppo, R. Sarode, S.B. Shurin, V. Chandrasekaran, S.P. Stabler, H. Sabio, E.E. Bouhassira, J.D. Upshaw Jr., D. Ginsburg, H.M. Tsai, Mutations in a member of the ADAMTS gene family cause thrombotic thrombocytopenic purpura, Nature 413 (2001) 488–494, http://dx.doi.org/10.1038/35097008.

[2] M. Furlan, R. Robles, M. Solenthaler, M. Wassmer, P. Sandoz, B. Lammle, Deficient activity of von Willebrand factor-cleaving protease in chronic relapsing thrombotic thrombocytopenic purpura, Blood 89 (1997) 3097–3103.

[3] M. Furlan, R. Robles, M. Solenthaler, B. Lammle, Acquired deficiency of von Willebrand factor-cleaving protease in a patient with thrombotic thrombocytopenic purpura, Blood 91 (1998) 2839–2846.

[4] M. Furlan, R. Robles, B. Lammle, Partial purification and characterization of a protease from human plasma cleaving von Willebrand factor to fragments produced by in vivo proteolysis, Blood 87 (1996) 4223–4234.

[5] H.M. Tsai, Physiologic cleavage of von Willebrand factor by a plasma protease is dependent on its conformation and requires calcium ion, Blood 87 (1996) 4235–4244.

[6] Z.A. Hing, T. Schiller, A. Wu, N. Hamasaki-Katagiri, E.B. Struble, E. Russek-Cohen, C. Kimchi-Sarfaty, Multiple in silico tools predict phenotypic manifestations in congenital thrombotic thrombocytopenic purpura, Br. J. Haematol. 160 (2013) 825–837, http://dx.doi.org/10.1111/bjh.12214.

[7] H.B. Feys, I. Pareyn, R. Vancraenbroeck, M. De Maeyer, H. Deckmyn, C. Van Geet, K. Vanhoorelbeke, Mutation of the H-bond acceptor S119 in the ADAMTS13 metalloprotease domain reduces secretion and substrate turnover in a patient with congenital thrombotic thrombocytopenic purpura, Blood 114 (2009) 4749–4752, http://dx.doi.org/10.1182/blood-2009-07-230615.

[8] A. Klukowska, E. Niewiadomska, U. Budde, F. Oyen, R. Schneppenheim, Difficulties in diagnosing congenital thrombotic thrombocytopenic purpura, J. Pediatr. Hematol. Oncol. 32 (2010) 103–107, http://dx.doi.org/10.1097/MPH.0b013e3181cbd265.

[9] Y. He, Y. Chen, Y. Zhao, Y. Zhang, W. Yang, Clinical study on five cases of thrombotic thrombocytopenic purpura complicating pregnancy, The Australian & New Zealand journal of obstetrics & gynaecology. 50 (2010) 519–522, http://dx.doi.org/10.1111/j.1479-828X.2010.01222.x.

[10] R. Rossio, B. Ferrari, A. Cairo, I. Mancini, G. Pisapia, G. Palazzo, F. Peyvandi, Two novel heterozygote missense mutations of the ADAMTS13 gene in a child with recurrent thrombotic thrombocytopenic purpura, Blood transfusion = Trasfusione del sangue 11 (2013) 241–244, http://dx.doi.org/10.2450/2012.0029-12.

[11] L.A. Lotta, H.M. Wu, I.J. Mackie, M. Noris, A. Veyradier, M.A. Scully, G. Remuzzi, P. Coppo, R. Liesner, R. Donadelli, C. Loirat, R.A. Gibbs, A. Horne, S. Yang, I. Garagiola, K.M. Musallam, F. Peyvandi, Residual plasmatic activity of ADAMTS13 is correlated with phenotype severity in congenital thrombotic thrombocytopenic purpura, Blood 120 (2012) 440–448, http://dx.doi.org/10.1182/blood-2012-01-403113.

[12] S.H. Lee, J.H. Park, S.K. Park, E.H. Lee, J.I. Choi, G.P. Visentin, T.S. Park, S.H. Oh, S.R. Kim, A novel homozygous missense ADAMTS13 mutation Y658C in a patient with recurrent thrombotic thrombocytopenic purpura, Ann. Clin. Lab. Sci. 41 (2011) 273–276.

[13] A. Borgi, M. Khemiri, A. Veyradier, K. Kazdaghli, S. Barsaoui, Congenital thrombotic thrombocytopenic purpura: atypical presentation and new ADAMTS 13 mutation in a Tunisian child, Mediterranean Journal of Hematology and Infectious Diseases 5 (2013), e2013041 http://dx.doi.org/10.4084/mjhid.2013.041.

[14] M. Bennett, Y. Chubar, I. Gavish, A. Aviv, G. Stemer, D. Chap-Marshak, Experiences in a family with the Upshaw-Schulman syndrome over a 44-year period, Clinical and Applied Thrombosis/Hemostasis: Official Journal of the International Academy of Clinical and Applied Thrombosis/Hemostasis, 20, 2014, pp. 296–303, http://dx.doi.org/10.1177/1076029613495309.

[15] C.U. Rank, J. Kremer Hovinga, M.M. Taleghani, B. Lammle, J.P. Gotze, O.J. Nielsen, Congenital thrombotic thrombocytopenic purpura caused by new compound heterozygous mutations of the ADAMTS13 gene, Eur. J. Haematol. 92 (2014) 168–171, http://dx.doi.org/10.1111/ejh.12197.

[16] E.S.K. Ma, Y.H. Li, J.S.Y. Kwok, S.C. Ling, P.W. Yau, G.C.F. Chan, ADAMTS13 mutational analysis in Chinese patients with chronic relapsing thrombotic thrombocytopenic purpura, Hong Kong Journal of Paediatrics. 11 (2006) 22–27.

[17] A. Metin, S. Unal, F. Gumruk, R. Palla, A. Cairo, M. Underwood, A. Gurgey, Congenital thrombotic thrombocytopenic purpura with novel mutations in three unrelated Turkish children, Pediatr. Blood Cancer 61 (2014) 558–561, http://dx.doi.org/10.1002/pbc.24764.

[18] M. Scully, M. Thomas, M. Underwood, H. Watson, K. Langley, R.S. Camilleri, A. Clark, D. Creagh, R. Rayment, V. McDonald, A. Roy, G. Evans, S. McGuckin, F. Ni Ainle, R. Maclean, W. Lester, M. Nash, R. Scott, P OB. Thrombotic thrombocytopenic purpura and pregnancy: presentation, management, and subsequent pregnancy outcomes, Blood 124 (2014) 211–219, http://dx.doi.org/10.1182/blood-2014-02-553131.

[19] T. Deal, J.A. Kremer Hovinga, M.B. Marques, J. Adamski, Novel ADAMTS13 mutations in an obstetric patient with Upshaw-Schulman syndrome, J. Clin. Apher. 28 (2013) 311–316, http://dx.doi.org/10.1002/jca.21251.

[20] L.A. Lotta, I. Garagiola, R. Palla, A. Cairo, F. Peyvandi, ADAMTS13 mutations and polymorphisms in congenital thrombotic thrombocytopenic purpura, Hum. Mutat. 31 (2010) 11–19, http://dx.doi.org/10.1002/humu.21143.

[21] R.S. Camilleri, M. Scully, M. Thomas, I.J. Mackie, R. Liesner, W.J. Chen, K. Manns, S.J. Machin, A phenotype-genotype correlation of ADAMTS13 mutations in congenital thrombotic thrombocytopenic purpura patients treated in the United Kingdom, Journal of thrombosis and haemostasis: JTH. 10 (2012) 1792–1801, http://dx.doi.org/10.1111/j.1538-7836.2012.04852.x.

[22] F. Taguchi, H. Yagi, M. Matsumoto, A. Sadamura, A. Isonishi, K. Soejima, Y. Fujimura, The homozygous p.C1024R- ADAMTS13 gene mutation links to a late-onset phenotype of Upshaw-Schulman syndrome in Japan, Thromb. Haemost. 107 (2012) 1003–1005, http://dx.doi.org/10.1160/th11-11-0799.

[23] E. Rurali, F. Banterla, R. Donadelli, E. Bresin, M. Galbusera, S. Gastoldi, F. Peyvandi, M. Underwood, G. Remuzzi, M. Noris, ADAMTS13 secretion and residual activity among patients with congenital thrombotic thrombocytopenic purpura with and without renal impairment, Clinical journal of the American Society of Nephrology: CJASN. 10 (2015) 2002–2012, http://dx.doi.org/10.2215/cjn.01700215.

[24] X. Zheng, D. Chung, T.K. Takayama, E.M. Majerus, J.E. Sadler, K. Fujikawa, Structure of von Willebrand factor-cleaving protease (ADAMTS13), a metalloprotease involved in thrombotic thrombocytopenic purpura, J. Biol. Chem. 276 (2001) 41059–41063, http://dx.doi.org/10.1074/jbc.C100515200.

[25] W. Gao, P.J. Anderson, E.M. Majerus, E.A. Tuley, J.E. Sadler, Exosite interactions contribute to tension-induced cleavage of von Willebrand factor by the antithrombotic ADAMTS13 metalloprotease, Proc. Natl. Acad. Sci. U. S. A. 103 (2006) 19099–19104, http://dx.doi.org/10.1073/pnas.0607264104.

[26] W. Gao, P.J. Anderson, J.E. Sadler, Extensive contacts between ADAMTS13 exosites and von Willebrand factor domain A2 contribute to substrate specificity, Blood 112 (2008) 1713–1719, http://dx.doi.org/10.1182/blood-2008-04-148759.

[27] S.Y. Jin, C.G. Skipwith, X.L. Zheng, Amino acid residues Arg(659), Arg(660), and Tyr(661) in the spacer domain of ADAMTS13 are critical for cleavage of von Willebrand factor, Blood 115 (2010) 2300–2310, http://dx.doi.org/10.1182/blood-2009-07-235101.

[28] I. Garagiola, C. Valsecchi, S. Lavoretano, H. Oren, M. Bohm, F. Peyvandi, Nonsense-mediated mRNA decay in the ADAMTS13 gene caused by a 29-nucleotide deletion, Haematologica 93 (2008) 1678–1685, http://dx.doi.org/10.3324/haematol.13102.

[29] H.B. Feys, M.T. Canciani, F. Peyvandi, H. Deckmyn, K. Vanhoorelbeke, P.M. Mannucci, ADAMTS13 activity to antigen ratio in physiological and pathological conditions associated with an increased risk of thrombosis, Br. J. Haematol. 138 (2007) 534–540, http://dx.doi.org/10.1111/j.1365-2141.2007.06688.x.

[30] K. Kokame, Y. Nobe, Y. Kokubo, A. Okayama, T. Miyata, FRETS-VWF73, a first fluorogenic substrate for ADAMTS13 assay, Br. J. Haematol. 129 (2005) 93–100, http://dx.doi.org/10.1111/j.1365-2141.2005.05420.x.

[31] I. Mackie, K. Langley, A. Chitolie, R. Liesner, M. Scully, S. Machin, F. Peyvandi, Discrepancies between ADAMTS13 activity assays in patients with thrombotic microangiopathies, Thromb. Haemost. 109 (2013) 488–496, http://dx.doi.org/10.1160/th12-08-0565.

[32] A.L. Barlow, A. Macleod, S. Noppen, J. Sanderson, C.J. Guerin, Colocalization analysis in fluorescence micrographs: verification of a more accurate calculation of pearson's correlation coefficient, Microscopy and Microanalysis: The Official Journal of Microscopy Society of America, Microbeam Analysis Society, Microscopical Society of Canada, 16, 2010, pp. 710–724, http://dx.doi.org/10.1017/s143192761009389x.

[33] E.M.M. Manders, F.J. Verbeek, J.A. Aten, Measurement of co-localization of objects in dual-colour confocal images, J. Microsc. 169 (1993) 375–382.

[34] D.H. Lee, A.L. Goldberg, Proteasome inhibitors: valuable new tools for cell biologists, Trends Cell Biol. 8 (1998) 397–403.

[35] E.J. Bowman, A. Siebers, K. Altendorf, Bafilomycins: a class of inhibitors of membrane ATPases from microorganisms, animal cells, and plant cells, Proc. Natl. Acad. Sci. U. S. A. 85 (1988) 7972–7976.

[36] C.R. Brown, L.Q. Hong-Brown, J. Biwersi, A.S. Verkman, W.J. Welch, Chemical chaperones correct the mutant phenotype of the delta F508 cystic fibrosis transmembrane conductance regulator protein, Cell Stress Chaperones 1 (1996) 117–125.

[37] B.K. Tamarappoo, B. Yang, A.S. Verkman, Misfolding of mutant aquaporin-2 water channels in nephrogenic diabetes insipidus, J. Biol. Chem. 274 (1999) 34825–34831.

[38] J.H. Robben, M. Sze, N.V. Knoers, P.M. Deen, Rescue of vasopressin V2 receptor mutants by chemical chaperones: specificity and mechanism, Mol. Biol. Cell 17 (2006) 379–386, http://dx.doi.org/10.1091/mbc.E05-06-0579.

[39] M. Akiyama, S. Takeda, K. Kokame, J. Takagi, T. Miyata, Crystal structures of the noncatalytic domains of ADAMTS13 reveal multiple discontinuous exosites for von Willebrand factor, Proc. Natl. Acad. Sci. U. S. A. 106 (2009) 19274–19279, http://dx.doi.org/10.1073/pnas.0909755106.

[40] I. Parmryd, J. Adler, R. Patel, A.I. Magee, Imaging metabolism of phosphatidylinositol 4,5-bisphosphate in T-cell GM1-enriched domains containing Ras proteins, Exp. Cell Res. 285 (2003) 27–38.

[41] J. Adler, S.N. Pagakis, I. Parmryd, Replicate-based noise corrected correlation for accurate measurements of colocalization, J. Microsc. 230 (2008) 121–133, http://dx.doi.org/10.1111/j.1365-2818.2008.01967.x.

[42] B. Tsai, Y. Ye, T.A. Rapoport, Retro-translocation of proteins from the endoplasmic reticulum into the cytosol, Nat. Rev. Mol. Cell Biol. 3 (2002) 246–255, http://dx.doi.org/10.1038/nrm780.

[43] M. Hunault, A.A. Arbini, J.A. Carew, F. Peyvandi, K.A. Bauer, Characterization of two naturally occurring mutations in the second epidermal growth factor-like domain of factor VII, Blood 93 (1999) 1237–1244.

[44] L. Canaff, J.F. Vanbellinghen, I. Kanazawa, H. Kwak, N. Garfield, L. Vautour, G.N. Hendy, Menin missense mutants encoded by the MEN1 gene that are targeted to the proteasome: restoration of expression and activity by CHIP siRNA, J. Clin. Endocrinol. Metab. 97 (2012) E282–E291, http://dx.doi.org/10.1210/jc.2011-0241.

[45] W.X. Ding, X.M. Yin, Sorting, recognition and activation of the misfolded protein degradation pathways through macroautophagy and the proteasome, Autophagy 4 (2008) 141–150.

[46] F. Engin, G.S. Hotamisligil, Restoring endoplasmic reticulum function by chemical chaperones: an emerging therapeutic approach for metabolic diseases, Diabetes Obes. Metab. 12 (Suppl 2) (2010) 108–115, http://dx.doi.org/10.1111/j.1463-1326.2010.01282.x.